PHYSICAL REVIEW VOLUME 188, NUMBER 1 5 DECEMBER 1969

Equilibrium Charge Distributions of C, N, Ar, and Fe in Carbon†

Peter L. Smith and Ward Whaling
California Institute of Technology, Pasadena, California 91109
(Received 1 July 1969)

The equilibrium charge distributions have been measured for carbon and argon in the energy range from 370 to 1450 keV, for iron in the energy range from 190 to 1450 keV, and for nitrogen from 180 to 1450 keV. Equilibrium was established by passing accelerated ions through 10 $\mu g/cm^2$ carbon foils. The ions of different charge were separated electrostatically and detected with a CsI(Tl) scintillator. Additional measurements were made to ensure that equilibrium had been achieved and that the effect of the residual gas was small. The values of the charge fractions are thought to be correct to within ±5% and agree well with the limited available data.

INTRODUCTION

Knowledge of the equilibrium charge distribution resulting from the passage of high-velocity ions through matter is useful in the planning and analysis of experiments in several fields. For example, in tandem accelerators, ions are stripped at the high-voltage terminal. Also, in energy-loss calculations, it is necessary to know the mean-squared charge on the stopped ion. Our particular interest is for beam-foil spectroscopy, in which the ion velocity is chosen to optimize production of the ionic state of interest. Also, the identification of the radiating ion is aided by the knowledge of the relative charge fractions and their variation with energy. There is no theory which allows one to calculate the charge distributions, although empirical formulas have been developed for use in fitting data.[1,2] Consequently, such equilibrium charge distributions must be measured experimentally.

EXPERIMENTAL METHOD

The apparatus is shown in Fig. 1. The ions were produced in a thermal source[3] in the high-voltage terminal of an electrostatic accelerator. The desired mass was selected by magnetic deflection, which bent the beam through 6°, followed by electrostatic deflection through 80° to measure and control the ion energy. The electrostatic analyzer was calibrated against the $^{19}F(p, \alpha\gamma)\,^{16}O$ resonance at 340.45 keV before and after the measurements. The uncertainty in the incident beam energy was ± 1%.

The beam passed through collimator A (0.05 × 0.84 mm) and then through a self-supporting carbon foil where the charge-state equilibrium was established. The supplier[4] quoted a foil thickness 10 ± 4 $\mu g/cm^2$ whereas our own measurements of the energy of the ions emerging from the foil, again by electrostatic deflection, are consistent with the energy loss in a foil of thickness 10 ± 2 $\mu g/cm^2$. To decrease straggling for iron beams of 200, 300, and 400 keV, 5 ± 3-$\mu g/cm^2$ foils were used. Collimator B (0.025 mm diam) defined a narrow beam which was then separated into the various charge components in an electric field. The particles were detected by two thin CsI(Tl) scintillators viewed by a Dumont 6291 phototube outside the vacuum. The distance from the foil to the scintillators was 29 cm. The pressure in the target chamber was less than 10^{-5} mm Hg at all times.

In order to avoid problems resulting from the fluctuations in the intensity of the ion beam, a series of alternating measurements of the number of particles in a given charge state and then of the number in the total beam were made, each for the same time interval. The sequence timer controlled this operation; gating the scalars, switching the voltage on the deflector plates, and blocking the neutral beam when a certain charge state was being measured. The cycle of measurements lasted 5 sec and was repeated three times for each value of the voltage on the deflector plates. As the deflector voltage was varied, each charge state was swept across the upper scintillator. A typical plot of the results is shown in Fig. 2. The neutral component was measured by selecting a deflector voltage at which no charge state hit the upper scintillator (e.g., at a value of 700 in Fig. 2) and by deactivating the chopper to allow the neutral component to strike the lower scintillator.

Preliminary attempts at such measurements employed surface-barrier detectors, including position-sensitive detectors. These proved to be unsatisfactory, at least for heavy ions such as iron and argon, because of energy loss and straggling in the gold window and because of the pulse-height defect for heavy ions. In addition, because

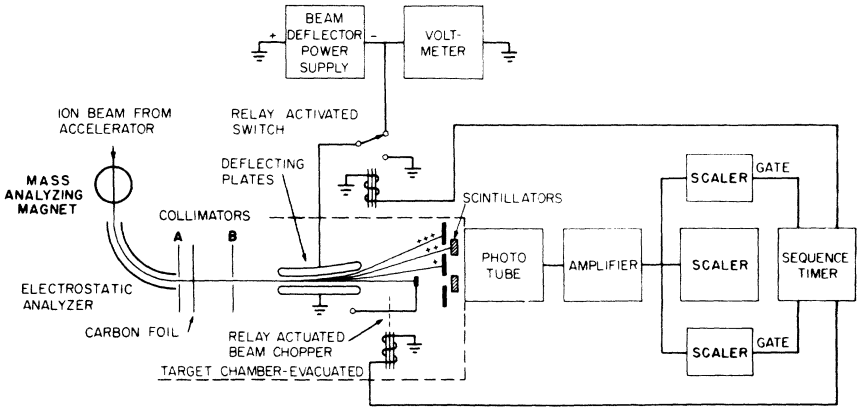

FIG. 1. Schematic diagram of charge-distribution measurement apparatus.

the beam collimators defined a very small area, the dose (or particles per unit area) quickly damaged the detector.

DISCUSSION OF RESULTS

The slit in front of the upper scintillator was considerably wider than the physical spread of the beam, which was determined by the collimators and by the variations in energy resulting from straggling in the foil. Consequently, the peaks in Fig. 2 have flat tops which give the values of the charge fractions. Note that the background was about 0.4%. It was generally less than 1% but significantly greater than the beam-independent background. When corrected for the small background, the sum of the charge fractions was seldom exactly unity, usually averaging about 0.98. Various explanations for the background and for the loss of beam were considered: charge-changing collisions with the residual-gas molecules, the decay of autoionizing levels, scattering from the residual gas or the deflector plates, extreme energy loss and straggling in the foil, and scattering from the edges of collimator B (a 0.025-mm hole punched in 0.0064-mm aluminum foil). Only the last explanation is consistent with the observation of a flat pressure-independent background.

The intensity of the beam from the accelerator was adjusted to give at least 1000 total beam counts per second in the undeflected beam or at least 6000 per point. As the average of all the points in the flat portion of the curve was used to compute the charge fraction, the statistical uncertainty was generally less than 1%. However, fluctuations in the accelerator beam current led to a much larger root-mean-square deviation from the average for the points in the flat portion of the curve. The relation $(\Delta P/P) \leq \pm 5\%$, where P is the charge fraction and ΔP is the rms deviation of the values which were averaged to give P,

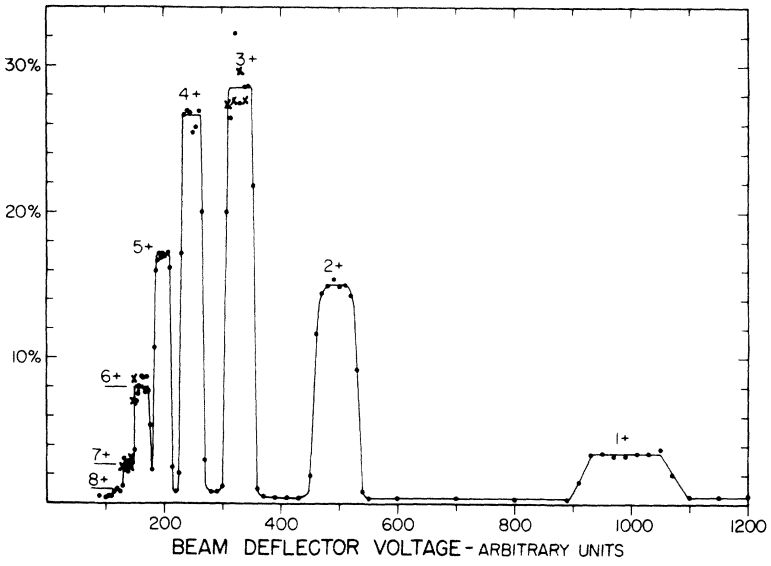

FIG. 2. Ratio of counts in upper scintillator to counts in lower scintillator as a function of the voltage on the deflector plates for argon at 1450-keV beam energy. The circles and crosses refer to separate sets of measurements. The curve is drawn to aid the eye.

TABLE I. Equilibrium charge fractions (%) as a function of emergent beam energy.

Iron										
Energy (keV)	190	289	388	468	566	664	761	957	1154	1450
Ion charge										
0	30.9 ± 1.7	20.7 ± 0.6	14.7 ± 0.5	10.9 ± 0.7	8.2 ± 0.7	5.1 ± 0.2	4.2 ± 0.3	1.9 ± 0.1	1.8 ± 0.2	0.3 ± 0.1
1	55.9 ± 3.0	53.4 ± 2.0	47.1 ± 0.7	41.6 ± 0.8	33.3 ± 1.2	25.9 ± 0.4	21.2 ± 0.8	12.7 ± 0.7	7.4 ± 0.8	3.5 ± 0.1
2	11.5 ± 1.0	19.7 ± 1.0	25.4 ± 1.2	28.1 ± 0.2	29.7 ± 0.9	29.5 ± 0.3	27.6 ± 0.7	21.9 ± 0.7	14.8 ± 1.5	8.9 ± 0.4
3	1.5 ± 0.1	4.9 ± 0.5	9.1 ± 0.6	12.6 ± 0.7	17.5 ± 0.6	21.1 ± 0.2	22.6 ± 0.4	24.3 ± 1.0	23.1 ± 1.0	16.7 ± 0.2
4	0.2 ± 0.1	1.1 ± 0.1	3.1 ± 0.1	5.3 ± 0.2	8.2 ± 0.3	12.3 ± 0.5	15.6 ± 0.4	20.8 ± 1.0	23.6 ± 1.4	26.0 ± 0.5
5		0.2 ± 0.1	0.6 ± 0.1	1.5 ± 0.1	2.8 ± 0.2	4.9 ± 0.2	6.9 ± 0.4	12.4 ± 0.4	17.2 ± 0.8	24.3 ± 0.7
6					0.4 ± 0.1	1.2 ± 0.1	1.7 ± 0.1	4.8 ± 0.4	8.7 ± 0.8	13.8 ± 0.7
7							0.2 ± 0.1	1.2 ± 0.1	2.6 ± 0.2	5.2 ± 0.2
8									0.6 ± 0.1	1.1 ± 0.1
9									0.2 ± 0.1	0.2 ± 0.1

Nitrogen									
Energy (keV)	180	275	373	465	567	713	960	1155	1450
Ion Charge									
0	44.5 ± 2.5	31.0 ± 2.2	18.2 ± 0.9	12.4 ± 0.4	8.2 ± 0.3	6.0 ± 0.2	2.2 ± 0.1	1.3 ± 0.1	0.3 ± 0.1
1	43.6 ± 2.7	46.8 ± 0.8	47.4 ± 0.6	43.4 ± 0.4	38.6 ± 1.2	32.2 ± 0.8	19.0 ± 0.4	12.8 ± 1.0	6.3 ± 0.1
2	11.1 ± 0.9	20.0 ± 1.2	28.8 ± 0.5	35.8 ± 1.7	40.7 ± 1.7	43.2 ± 0.5	43.7 ± 0.6	39.8 ± 1.9	32.6 ± 0.4
3	0.7 ± 0.1	2.2 ± 0.1	4.5 ± 0.2	8.1 ± 0.3	11.7 ± 0.4	16.9 ± 0.5	30.0 ± 1.2	38.1 ± 2.8	45.8 ± 0.5
4			0.1 ± 0.1	0.4 ± 0.1	0.8 ± 0.1	1.5 ± 0.1	4.8 ± 0.3	7.5 ± 0.6	13.8 ± 0.1
5						1.1 ± 0.1	0.3 ± 0.1	0.5 ± 0.1	1.2 ± 0.1

Argon								
Energy (keV)	372	469	566	762	958	1155	1450
Ion charge							
0	7.5 ± 0.5	4.8 ± 0.4	3.4 ± 0.3	1.5 ± 0.1	0 ± 0.1	0 ± 0.1	0 ± 0.1
1	35.0 ± 1.9	26.7 ± 0.8	22.9 ± 1.2	14.4 ± 0.4	8.7 ± 0.2	5.9 ± 0.3	3.1 ± 0.2
2	31.9 ± 1.5	33.8 ± 1.0	33.2 ± 1.8	30.2 ± 1.0	25.5 ± 0.7	20.3 ± 0.6	15.0 ± 0.2
3	18.4 ± 0.9	23.0 ± 0.7	25.5 ± 1.7	29.8 ± 0.7	32.7 ± 0.9	31.3 ± 0.5	28.6 ± 1.7
4	5.9 ± 0.3	8.8 ± 0.2	10.8 ± 1.2	15.7 ± 1.0	20.3 ± 0.4	23.8 ± 0.5	26.2 ± 0.6
5	1.3 ± 0.1	2.3 ± 0.4	3.4 ± 0.2	6.2 ± 0.2	8.8 ± 0.3	12.4 ± 0.4	16.9 ± 0.2
6	0.1 ± 0.1	0.5 ± 0.1	0.8 ± 0.1	1.7 ± 0.2	3.1 ± 0.1	5.0 ± 0.3	7.6 ± 0.4
7				0.4 ± 0.1	0.8 ± 0.1	1.2 ± 0.1	2.2 ± 0.3
8						0.1 ± 0.1	0.5 ± 0.1

Carbon							
Energy (keV)	369	470	567	762	960	1156	1450
Ion charge							
0	18.7 ± 0.6	12.7 ± 0.3	10.0 ± 0.3	4.5 ± 0.4	2.5 ± 0.6	1.0 ± 0.1	0.4 ± 0.2
1	51.0 ± 0.3	48.1 ± 2.3	43.1 ± 2.0	33.8 ± 1.9	23.8 ± 2.0	16.1 ± 0.7	8.3 ± 0.5
2	27.3 ± 0.9	34.4 ± 2.1	39.6 ± 1.3	47.7 ± 2.0	50.6 ± 4.1	49.7 ± 2.4	43.1 ± 2.8
3	2.9 ± 0.2	4.6 ± 0.2	6.7 ± 0.8	13.0 ± 0.5	20.8 ± 1.6	29.2 ± 1.9	40.6 ± 1.4
4	0.1 ± 0.1	0.1 ± 0.1	0.6 ± 0.1	1.0 ± 0.2	2.4 ± 0.2	4.0 ± 0.2	7.5 ± 0.3

holds for two-thirds of the values for which $P \geq 10\%$. Thus, we think that the measured values of the charge fractions are accurate to $\pm 5\%$ of their values (i.e., $P \pm 0.05P$).

Corrections were made for the energy loss in the foil following a theoretical treatment by Lindhard, Scharff, and Schiott.[5] Only the electronic stopping term was considered because the particles which passed through the collimators were not those which had undergone large-angle nuclear scatterings. The results are tabulated in Table I.

Various studies were made to determine the effect of the beam on the foils. The energy loss in the foil was observed to increase by about 50% after 2 h of bombardment. Normally, the foils were used for about 5 min.

For iron with beam energies of 700 and 1500 keV and for nitrogen with a beam energy of 1400 keV, foils of both 10 and 20 $\mu g/cm^2$ thickness were used. When corrected for energy loss, the data were consistent for the two foils, indicating that equilibrium had been established in the thinner foil.

COMPARISON WITH OTHER MEASUREMENTS

There are few data available in the literature for these ions in this energy range. Seeger and Kavanagh[6] have published data for carbon in VN from 1.65 to 3.5 MeV. Our data extrapolate smoothly to fit theirs. There are no data for iron.

There are data for celluloid targets at 680 and 1220 keV with a nitrogen beam and at 1400 keV with an argon beam.[7] Comparison with our results is shown in Table II and, for nitrogen only, in Fig. 3. The agreement is within the uncertainty of the values which are taken from the graphs in Ref. 7. The dependence on foil material is not expected to be significant.[1]

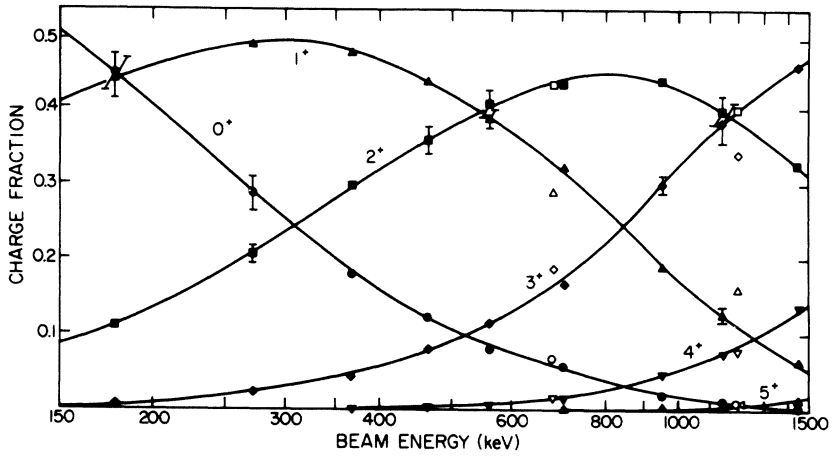

FIG. 3. Equilibrium charge distribution for nitrogen in carbon foils. The open symbols refer to data from Ref. 7. Root-mean-square deviations less than ±0.02 are not shown. The curves are drawn to aid the eye.

TABLE II. Comparison of present measurements in carbon foils with those of Nikolaev *et al.* (Ref. 7) in celluloid. California Institute of Technology (Caltech) values are taken from smooth curves through experimental points listed in Table I.

Charge	Argon 1400 keV		Nitrogen 680 keV		Nitrogen 1220 keV	
	Caltech	Ref. 7	Caltech	Ref. 7	Caltech	Ref. 7
0	0.0	0	6.0	7	1.0	1
1	3.3	3	32.5	29	11.2	16
2	15.3	15	43.2	43	38.4	40
3	28.8	29	16.6	19	39.9	34
4	26.1	27	1.7	2	8.7	8
5	16.3	15			0.8	1
6	7.4	8				
7	2.3	3				
8	0.5					

†Supported in part by the National Science Foundation (GP-9114) and the Office of Naval Research [Nonr-220 (47); Nonr-220(49)].

[1]C. S. Zaidins, California Institute of Technology, 1962 (unpublished) [a somewhat condensed version of this report may be found in J. B. Marion and F. C. Young, Nuclear Reaction Analysis (North-Holland Publishing Co., Amsterdam, 1968)]; Ph.D. thesis, California Institute of Technology, 1967 (unpublished), Appendix I.

[2]I. S. Dmitriev and V. S. Nikolaev, Zh. Eksperim. i Teor. Fiz. 47, 615 (1964) [English transl.: Soviet Phys. – JETP 20, 409 (1965)].

[3]G. D. Magnuson, C. E. Carlston, P. Mahadevan, and A. R. Comeaux, Rev. Sci. Instr. 36, 136 (1965).

[4]Yissum Research Development Company, Hebrew University, Jerusalem, Israel.

[5]J. Lindhard, M. Scharff, and H. E. Schiott, Kgl. Danske Videnskab. Selskab, Mat.-Fys. Medd. 33, No. 14 (1963).

[6]P. A. Seeger and R. W. Kavanagh, Nucl. Phys. 46, 577 (1963).

[7]V. S. Nikolaev, I. S. Dmitriev, L. N. Fateeva, and Ya. A. Teplova, Zh. Eksperim. i Teor. Fiz. 39, 627 (1961) [English transl.: Soviet Phys. – JETP 12, 627 (1961)].

PHYSICAL REVIEW VOLUME 188, NUMBER 1 5 DECEMBER 1969

Pressure Effects of Foreign Gases on the Absorption Lines of Cesium. VI. Intensity Measurements of the Cesium Resonance Lines and Their Associated Satellites in the Presence of Various Foreign Gases*

David E. Gilbert† and Shang Yi Ch'en
Physics Department, University of Oregon, Eugene, Oregon 97403
(Received 7 July 1969)

The intensity contours of the pressure-broadened Cs resonance lines and their associated satellites in the presence of He, Ne, Ar, Kr, Xe, and CF_4 are studied. The total integrated intensity of the lines and satellites in the presence of these gases is found to decrease exponentially with the relative density (rd) of foreign gas. For the range of foreign-gas pressures studied (0 to ~50 rd), the ratio of the integrated intensity of the $^2P_{3/2}$ component to that of the $^2P_{1/2}$ component is found to be close to the theoretical value of 2 for all rd's only when the integrated intensity of the satellites is included with the parent lines. These ratios (1.90 ± 0.03 for Ar, 2.00 ± 0.03 for Kr, and 2.06 ± 0.04 for Xe) indicate that satellites are part of the lines. The integrated intensity of the violet satellites associated with the $^2P_{3/2}$ component in the presence of these gases is found to be proportional to the cube of the low-energy collision diameter of the particular foreign gas. A violet satellite associated with the $^2P_{1/2}$ component is observed in the presence of CF_4.

I. INTRODUCTION

When an optical atom is placed in a foreign gas, not only are the frequencies and widths of its spectral lines modified, but satellite bands usually appear in the neighborhood of the first few members of the spectral line series.[1] For alkali atoms, such as Cs, red satellites appear on the red side of each component of the first few principal series doublets if the foreign gas used produces a red shift of the spectral lines. Also, a satellite usually appears on the violet side of the $^2P_{3/2}$ component of the resonance lines (the first doublet of the absorption series) for all foreign gases. The separation between the violet satellite and the resonance line is much greater than that for the red satellites, but the corresponding separation for the case of the second doublet decreases so rapidly that the violet satellite is resolvable only for light gases.

Although several hundred satellites of this nature have been observed, there was no adequate intensity data. With the addition of a dual-beam system employing photomultiplier output and phase-sensitive detection along with electronic log conversion to our 35′ grating spectrograph, it is possible to obtain, as direct output, a plot of the absorption coefficient as a function of wavelength. The background intensity is flat over a wide range in wavelengths, so intensity informa-